Ecological Indicators 93 (2018) 804–812

Contents lists available at ScienceDirect

Ecological Indicators

journal homepage: www.elsevier.com/locate/ecolind

Original Articles

Vegetation changes in the Three-River Headwaters Region of the Tibetan Plateau of China

Xiaoji Shen[a,b], Ru An[a,*], Li Feng[a], Nan Ye[b], Liujun Zhu[b], Maohua Li[a]

[a] Department of Geographic Information Science, Hohai University, Nanjing 211100, China
[b] Department of Civil Engineering, Monash University, Clayton, Victoria 3800, Australia

ARTICLE INFO

Keywords:
Vegetation change
Time series analysis
DBEST
TRHR
NDVI
MODIS

ABSTRACT

The Three-River Headwaters Region (TRHR), located in the hinterland of the Tibetan Plateau, is a key ecological region of China for its abundant natural resources and crucial ecological functions. In recent decades, severe vegetation degradation is observed due to its fragile ecosystems, global climate change and frequent human disturbance. To restrain the further degradation, the Chinese government initiated an ecological conservation project of TRHR in 2005 with a total investment of around 1 billion USD. Here, the vegetation changes during 2000–2015 as well as the effects of the ecological conservation project were investigated using Moderate Resolution Imaging Spectroradiometer (MODIS) Normalized Difference Vegetation Index (NDVI) time series and a generic approach for vegetation trend analysis, Detecting Breakpoints and Estimating Segments in Trend (DBEST). The results show that the vegetation of TRHR underwent an overall recovery with NDVI trend from around 0.24 in 2000 to 0.26 in 2015. The project was proved to have a positive but insignificant effect on the vegetation recovery based on the comparison of the vegetation changes inside and outside the reserve from 2005 to 2015. However, TRHR is still at a risk of further degradation because increasing fluctuations in trend were also observed. Significant degradation was found in reserves including Dongzhong, Aangsai, Baizha, Tongtian River and Nianbaoyuze. It is suggested that long-term vegetation and ecosystem conservation efforts remain to be continuously conducted particularly in the aforementioned areas. This study provides knowledge for future ecosystem conservation of TRHR, and also enriches the remotely sensed detection of the vegetation changes.

1. Introduction

The Three-River Headwaters Region (TRHR), located in the hinterland of the Tibetan Plateau, is the source region of Yangtze, Yellow and Lancang Rivers. The TRHR has significant conservation and regulation functions of water resources (Shao et al., 2017a). It supplies 25%, 49% and 15% of the total water for the three rivers, respectively (Zhang et al., 2012), and its annual average runoff reaches around 40 billion m^3 (Shao et al., 2017b). Accordingly, the TRHR is termed as the "Chinese Water Tower." Special location, abundant natural resources and crucial ecological functions make it an important ecological barrier of the Tibetan Plateau in China (Shao et al., 2017a).

However, the TRHR faces severe vegetation degradation (e.g. grassland degradation showed in Fig. S1), soil erosion, desertification, glacier retreat, lake and wetland decline and so on (Liu et al., 2008; Shao et al., 2009; Zhang et al., 2012) because of its fragile ecosystem, climate change and increasing human activities in recent decades. This poses a serious threat to the ecological and economic development both in this area and also its downstream regions. To restrain the further degradation of the TRHR, the Chinese government carried out the 'The general planning on ecological conservation and restoration in the TRHR reserve in Qinghai Province' (referred as 'The Project' hereafter) in 2005 (PGQP, 2013). The first stage of 'The Project' was implemented from 2005 to 2012 with an investment of approximately 1 billion USD, aiming at improving the vegetation cover through conserving grassland, forest and wetland (Shao et al., 2017a). The second stage has started in 2013 and will end in 2020 with a total supposed investment of 2.4 billion USD (PGQP, 2013; Zhao, 2014).

Vegetation is the principal component of the ecosystem of TRHR and covers over 70% of its total area, mainly consisting of grassland, forest, cropland and part of wetland (Xu et al., 2008). It is the most sensitive component to climate change (Parmesan and Yohe, 2003; Sitch et al., 2003) and its changes are closely associated with livestock breeding, deforestation and desertification monitoring and anthropogenic activities (Purevdorj et al., 1998). To this end, the detection of long-term vegetation changes in this area has been attracting considerable attention from the scientific community (Li et al., 2011; Liu et al., 2014; Liu and Shao, 2014; Sun et al., 2016; Zhang et al., 2016),

* Corresponding author.
E-mail address: anrunj@163.com (R. An).

https://doi.org/10.1016/j.ecolind.2018.05.065
Received 4 January 2018; Received in revised form 9 March 2018; Accepted 25 May 2018
Available online 01 June 2018
1470-160X/ © 2018 Elsevier Ltd. All rights reserved.

and so has the assessment of 'The Project' on vegetation changes (Cai et al., 2015; Jiang and Zhang, 2016; Shao et al., 2017a). Li et al. (2011) analyzed SPOT VEGETATION Normalized Difference Vegetation Index (NDVI) data and found the vegetation in TRHR showed an increasing trend in density from 2001 to 2010. Zhang et al. (2016) estimated the net primary productivity (NPP) of TRHR from 1982 to 2012, and the average NPP exhibited a generally increasing but fluctuated tendency. Cai et al. (2015) used SPOT NDVI-based residual trend as an indicator, and they revealed 'The Project' mitigated the grassland degradation and even reversed it in some areas.

However, the methods used in these studies are mainly linear regression based on least-square fit, which may obscure changes appearing within short duration (de Jong et al., 2012). Accordingly, new tools for analyzing vegetation time series were proposed such as Detecting Breakpoints and Estimating Segments in Trend (DBEST) (Jamali et al., 2015). de Jong et al. (2012) concluded that such new tools for 'automatic detection' is more promising in the analysis of long-term vegetation changes. DBEST accounts for seasonal variation and decomposes time series into trend (low frequency variation), seasonality (variation at or near the seasonal frequency) and remainder. It is flexible since it allows users to completely control either fine details or general features of the trend to be captured.

In this study, we aim at detecting the vegetation changes of TRHR and further assessing the effects of 'The Project' on vegetation changes using DBEST, which to our knowledge is the first application of DBEST in this region. Both generalized long-term trend and fine short-term fluctuations were characterized, which can be hardly implemented by linear methods. This study includes three components: 1) in Section 4.1, vegetation trend of the entire TRHR and the change magnitude for each pixel were analyzed to show the long-term aggregated changes; 2) in Section 4.2, the major vegetation change was detected to reflect the short-term changes probably caused by specific events (e.g. wildfires, flood and earthquake etc.); and 3) in Section 4.3, the effectiveness of 'The Project' on the vegetation recovery was assessed through a comparison of the vegetation changes inside and outside the reserve.

2. Data and study area

2.1. Data

The ten-day MODND1T NDVI product used in this study was downloaded from the Geospatial Data Cloud (http://www.gscloud.cn/). It was calculated from daily Terra-MODIS (Terra-Moderate Resolution Imaging Spectroradiometer) MOD09GA surface reflectance dataset (Vermote et al., 2011) and was aggregated from the ten-day maximum composites in time. It covers the whole China at 500 m spatial resolution. The time span covers from February 2000 to May 2016 except some unavailable records between 2015 and 2016. Thus, a total of 540 NDVI images from the third ten-day of February 2000 to the second ten-day of February 2015 were used.

The land use/cover dataset of China was downloaded from the Chinese Academy of Environmental Science data center (http://www.resdc.cn) (Liu, 1997). This dataset was produced by visually interpreting Landsat TM/ETM images. It covers years of 1990, 1995, 2000, 2005, 2010 and 2015 and its spatial resolution is 1 km. In this study, the map of 2010 was used to provide water boundary to exclude non-vegetation area (please refer to Section 3.2).

2.2. Study area

The TRHR is the source region of Yangtze, Yellow, and Lancang Rivers and thus referred to as the "Chinese Water Tower." It is located in the hinterland of the Tibetan Plateau, Qinghai province, China (Fig. 1). The TRHR has an area of approximately 363,000 km^2, including 16 counties and Tanggulashan Township (Shao et al., 2017b). It is the largest reserve (~152,300 km^2) in China with 18 reserve subregions where 'The Project' was implemented (Shao et al., 2017b). As the world's largest alpine wetland ecosystem, the TRHR has rich rivers, lakes, mountain snow and even glaciers to supply water for the downstream regions (Tong et al., 2014). Its annual average runoff is around 40 billion m^3 (Shao et al., 2017b) and incorporates 25%, 49% and 15% of the runoff of Yangtze, Yellow, and Lancang River Basins, respectively (Zhang et al., 2012). The main land cover includes grassland, wetland, forest, crop, desert and other type accounting for 65.37%, 8.40%, 4.71%, 0.25%, 8.57% and 12.70%, respectively. There are 69 species of national protected animals in the TRHR, including 17 level-I and 52 level-II species (PGQP, 2013).

The high elevation, cold and dry climate and intense radiation in TRHR make it an ecologically sensitive region (Jiang and Zhang, 2016; Xu et al., 2011). The climate dries and the elevation increases from southeast to northwest (Tang et al., 2016), resulting in a better climate condition of the southeast. This corresponds well with the tendency of

Fig. 1. The location, administrative regions, reserves and the mean NDVI of TRHR. The mean NDVI was calculated by averaging the 540 NDVI images from the third ten-day of February 2000 to the second ten-day of February 2015. The non-vegetation area is masked.

the mean NDVI which decreases from 0.72 in the east to 0 in the west (Fig. 1). The elevation ranges from 1987.5 m to 6714.5 m with an average over 4000 m (Jiang and Zhang, 2016). The annual average temperature is between −5.6 and 7.8 °C and the annual rainfall ranges from 262.2 to 772.8 mm (PGQP, 2013). In recent decades, global climate warming and increasing human activities have led to severe ecological degradation in the TRHR including vegetation degradation, glacier retreat, the rising snow line, soil and water loss etc. (Liu et al., 2008; Shao et al., 2009; Zhang et al., 2012).

3. Methodology

3.1. DBEST

Fig. S2 briefly shows the workflow of DBEST including trend extraction as well as trend segmentation and modeling. Please refer to Jamali et al. (2015) for more details. Trend extraction is performed using STL (Seasonal-Trend decomposition procedure based on Loess) which is able to decompose the original vegetation index (VI) time series into three components with the same physical meaning and unit, i.e. trend, seasonality and remainder (Cleveland and Cleveland, 1990). Prior to performing STL, abrupt changes called *level-shift points* are detected first based on three user-defined thresholds including θ_1, θ_2 and ϕ (Table 1). A point p_i is identified as a *level-shift point* if it meets three conditions: 1) the absolute difference of p_i and its successive point p_{i+1} is larger than θ_1; 2) the absolute difference in the means of the VI, calculated over ϕ before and after the current time step i, is greater than θ_2; and 3) the spacing between p_i and any other *level-shift point* is at least ϕ. STL decomposition is then successively performed on sub-series separated by *level-shift points* and the original trend time series is extracted.

For the extracted trend time series, the *peak/valley points*, *turning points* are firstly found. Next, *trend local change* is calculated by subtracting the VI value at the current *turning point* from the next *turning point*. All u *turning points* are sorted into descending order according to their *trend local changes*, and then they are added one by one to model the trend time series using piecewise linear regression. Bayesian Information Criterion (BIC) (Schwarz, 1978) is simultaneously computed for each modeling. When BIC is minimum, the s *turning points* ($s \leq u$) are considered breakpoints and the model trend composed of linear segments is obtained.

DBEST provides two applications for trend modeling to be selected by users: trend generalization and change detection. With trend generalization, users are allowed to control the number of the breakpoints (less than s) included in the model trend using m, β and δ (Table 1). $m = 0$, $\beta = 1$ and $\delta = 100\%$ denote no breakpoint is included and a straight line will be generalized. $m > 0$, $\beta < 1$ and $\delta < 100\%$ denote possible breakpoints are included and a composite line will be obtained. The outputs of the trend generalization are the model trend, number of segments, and fit quality measures.

As for change detection, all of the s breakpoints are included in the model trend and a composite line with all significant vegetation changes will be obtained. Users can only control the number of the breakpoints on display using m and β. The outputs of change detection are start time, end time, change duration, change magnitude, change type and significance. Every breakpoint is the start of a vegetation change event, and the next breakpoint is the end. Start time and end time are the steps of the two consecutive breakpoints, respectively. Change duration is the steps between the two breakpoints, and the change magnitude is the VI value calculated by subtracting the start point from the end point. Change type denotes whether the change is abrupt or non-abrupt. Significance denotes if the corresponding segment of the change computed by the regression model is statistically significant. In this study, mainly change detection was adopted if not specified.

3.2. Analysis of NDVI changes

The non-vegetation area should be removed first. Different from the average NDVI threshold of 0.1 used in Jamali et al. (2014), a maximum NDVI threshold of 0.2 was employed suggested by Gu et al. (2010) and Montandon and Small (2008), to include the 'possible vegetation area'. This may help include the transition areas whose landcover changes in the period of interest. In addition, the pixels with NaN values in time series or with water land cover were masked (Fig. 1).

To get the long-term aggregated vegetation changes, accumulated change magnitude (ACM) was computed according to de Jong et al. (2012). DBEST was successively performed on all pixels, and the values of all significant changes were summed up to the ACM for each pixel. The user-defined thresholds were set according to the private suggestion by the authors of DBEST. Specifically, θ_1, θ_2 and α were kept default values of 0.1, 0.2 and 0.05, respectively. Seasonal period was set at 36 ten-day which is roughly one year; and ϕ was set at double seasonal periods, that is 72 ten-day. ε was estimated automatically by the DBEST program (Jamali et al., 2015).

4. Results

General vegetation change was characterized by temporal trend and the spatial distribution of ACM over TRHR, to show the changes throughout the entire study period. Differing from general vegetation change, major vegetation change, the change with maximum change magnitude for each time series, could reflect fine short-term fluctuations.

4.1. General vegetation change

Fig. 2a shows the decomposition of the averaged NDVI time series of TRHR into seasonality, trend and remainder, and no abrupt change was detected. Fig. 2b shows the model trends using trend generalization and change detection. The model trend using trend generalization (red line) grew steadily from 0.24 in 2000 to 0.26 in 2015, indicating an overall

Table 1
The user-defined thresholds in DBEST (adapted from Jamali et al. (2015)).

Threshold	Description
θ_1 (First level-shift-threshold)	The lowest absolute difference in VI values between the level-shift point and the next point
ϕ (Duration-threshold)	The lowest time period within which the shift in the means of the data level, before and after the level-shift point, persists; and, the lowest spacing (time steps) between successive level-shift points
θ_2 (Second level-shift-threshold)	The lowest absolute difference in the means of the data calculated over the period ϕ before and after the level-shift point
ε (Distance-threshold)	The lowest perpendicular distance from farthest data point to the straight line passing through every pair of successive peak and valley points
m (Change number)	Number of breakpoints included in the model trend for trend generalization; number of breakpoints of interest for change detection
β (Change magnitude)	The lowest magnitude of breakpoints included in the model trend for trend generalization; the lowest magnitude of breakpoints of interest for change detection
δ (Generalization-threshold)	Generalization level (trend generalization): 0 for all and 100% for none of breakpoints are included in the model trend
α (Statistical significance level)	Statistical significance level used for testing significance of detected changes

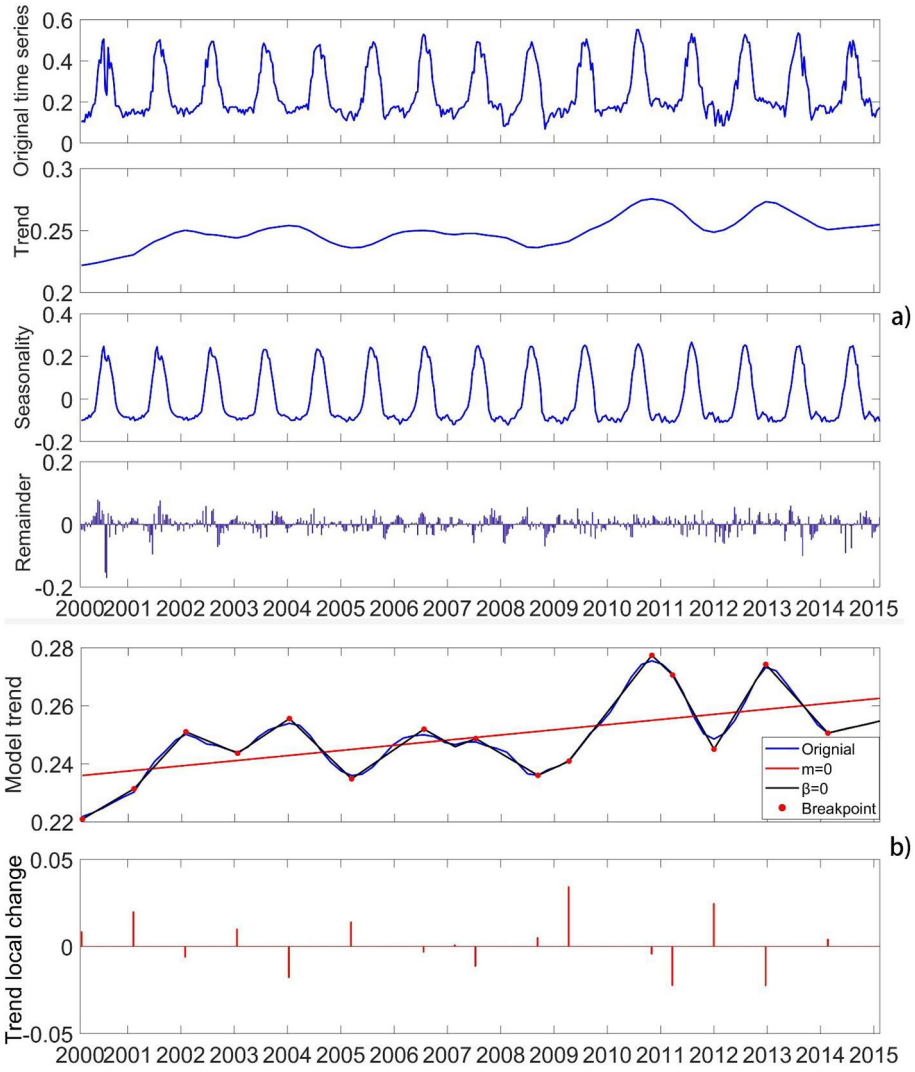

Fig. 2. (a) Decomposition and trend extraction of the averaged NDVI time series of TRHR. (b) Model trends with breakpoints. The blue line is the original trend extracted as showed in (a). The black and red lines are derived from change detection with $\beta = 0$ and trend generalization with $m = 0$, respectively. The trend local change shows the change magnitude of corresponding breakpoint. (For interpretation of the references to colour in this figure legend, the reader is referred to the web version of this article.)

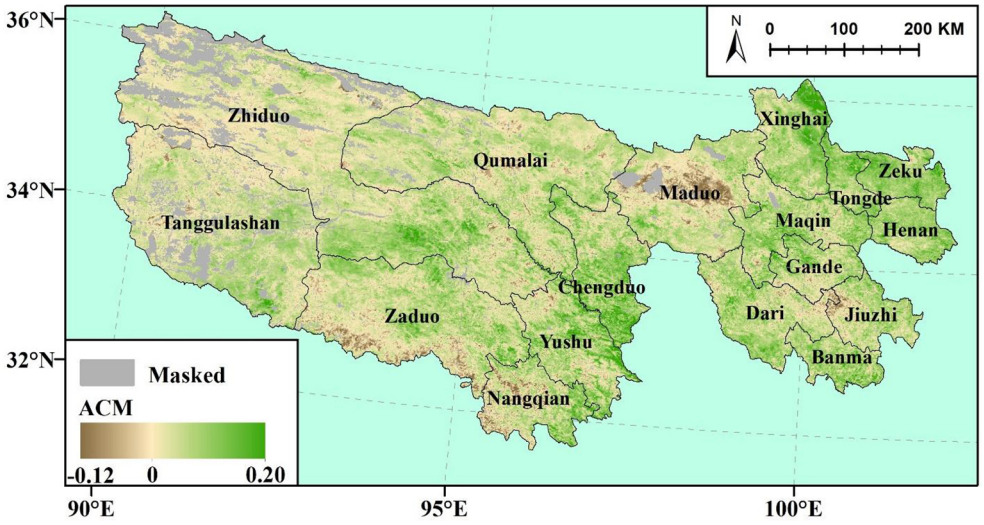

Fig. 3. The accumulated change magnitude (ACM) of TRHR.

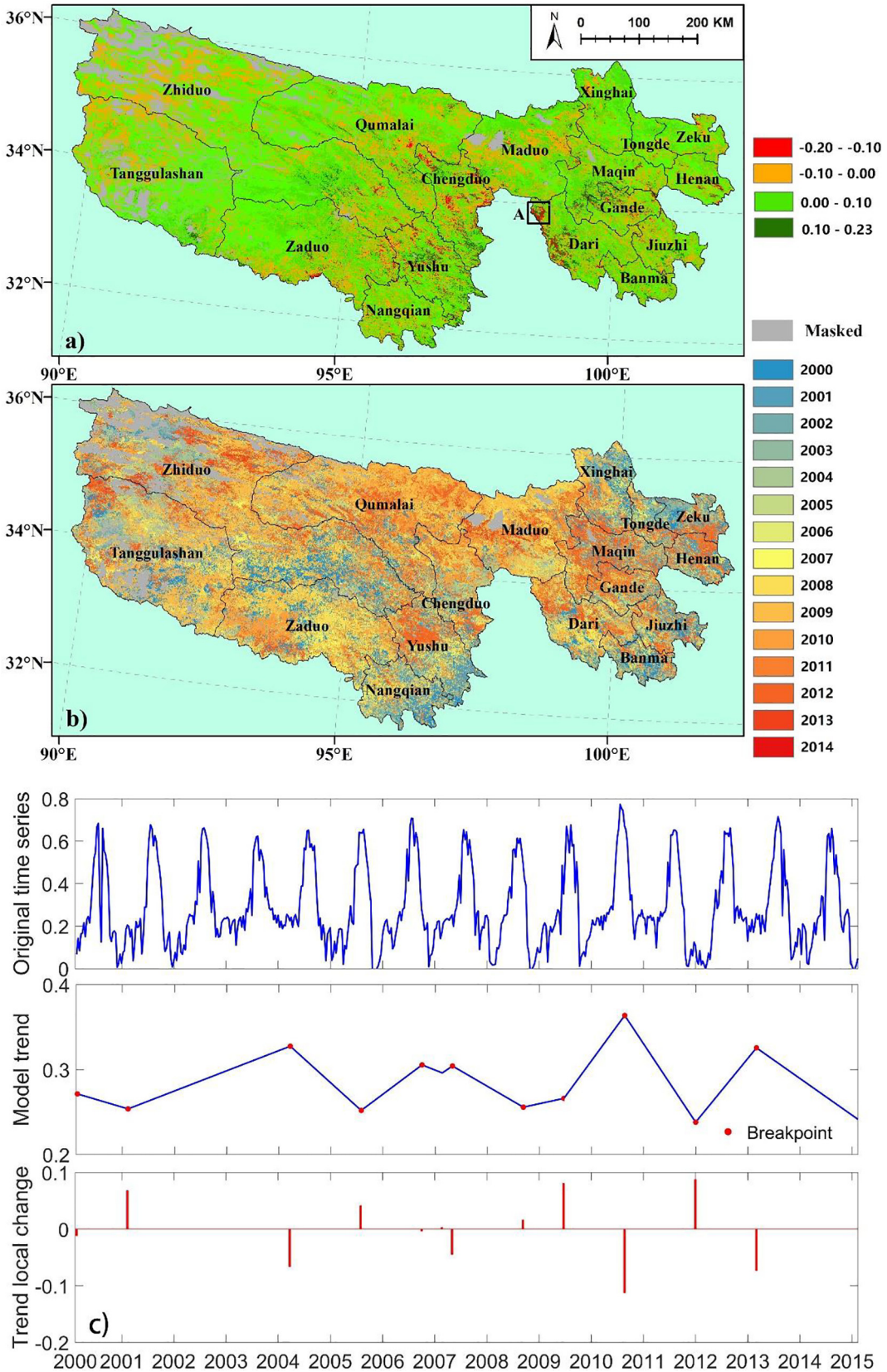

Fig. 4. (a) The change magnitude and (b) the start time of the major vegetation changes over TRHR. (c) The averaged time series and the model trend of the pixels with values less than −0.10 (in red) in 'Region A' marked in (a). The trend local change shows the change magnitude of corresponding breakpoint. (For interpretation of the references to colour in this figure legend, the reader is referred to the web version of this article.)

recovery of the vegetation. Despite the overall recovery, significant progressive fluctuations were observed from the model trend using change detection (black line). The trend started with the lowest level of 0.22 in 2000. After two M-shape fluctuations in 2000–2005 and 2005–2008, it rose rapidly in 2009 and 2010 and reached the peak closing to 0.28. Although the trend fluctuated drastically later, it kept a relatively high level of around 0.25 in 2014 and 2015.

Fig. 3 shows the distribution of ACM varying from −0.12 to 0.20, and the average ACM is 0.033. Pixels with positive ACM account for 89.38% of the total valid pixels, indicating around 90% areas were recovered. Obviously recovered areas (ACM ~ 0.20) are distributed primarily in the southeastern TRHR, including Xinghai, Tongde, Zeku, as well as the middle regions, such as Chengduo and Yushu. In addition, the vegetation in the east shows a more significant tendency of recovery than that in the west. This can be attributed to the relatively low elevation and humid climate in the east, which has been stated in Section 2.2. Degraded areas are mainly located in Maduo, Zaduo, Nangqian, Jiuzhi and Zhiduo. From the temporal trend and spatial distribution of vegetation changes, we may conclude that the vegetation of TRHR generally recovered with fluctuations during the study period.

4.2. Major vegetation change

DBEST was successively performed on all pixels and the change magnitude as well as the start time of the major change was obtained (Fig. 4a and b). All the major changes in the figure are significant and no abrupt change was detected. From Fig. 4a we can clearly observe that most changes are positive with relatively little absolute values ranging from 0 to 0.10. The major degradation is primarily distributed in the middle TRHR including Qumalai, Maduo, Yushu and Chengduo, as well as in the western TRHR such as Zhiduo, Zaduo and Tanggulashan. Fig. 4b indicates that the major changes occurred from time to time but more frequently after around 2009 (orange and red), confirming the intense fluctuation since 2009 which was found in Section 4.1.

Particularly, a cluster of pixels with change magnitude less than −0.10 are captured in the 'Region A' in Dari (Fig. 4a). A further investigation was performed on its averaged time series of all the pixels with values less than −0.10 (in red) (Fig. 4a and c). The results show the overall level of the original time series is high, especially in 2010 when it reached the peak closing to 0.8. Since then, however, the trend declined sharply to around 0.23 in 2012. Although it picked up later, it finally fell back to the level of 2012. Extraordinary coincidence is that this model trend has almost the same 'M-shape' fluctuation from 2009 to 2015 as the TRHR trend (Fig. 2b). Despite lack of convincing proof, we speculate an intense climate fluctuation occurred over the TRHR, involving 'Region A' and resulting in their similar 'M-shape' fluctuations.

4.3. The effect of 'The Project' on the vegetation recovery

In this section, we compared the ACMs inside and outside the reserve, from the third ten-day of February 2005 to the second ten-day of February 2015 covering the implementation of 'The Project', to assess the effectiveness of 'The Project' on the vegetation recovery. Fig. 5 shows the ACM of TRHR varies spatially from −0.16 to +0.16. The vegetation gennerally recovered in the east, degraded in the middle and remained unchanged in the west. Significant recoveries are distributed mainly in the north of Xinghai, Banma and Maduo. Severe degradation is observed not only in reserves including Dongzhong, Baizha and Tongtian River, but also in non-reserve, that is the border area of Zhiduo, Qumalai, Yushu and Zaduo.

The ACMs of 18 reserves were averaged and depicted in Fig. 6. We can note that the top four degraded reserves are Dongzhong, Angsai, Baizha and Tongtian River. Coincidentally, they are all located in the south of the middle TRHR. Make River, Duoke River, Yueguzonglie, Zhongtiejungong, Xingxinghai and Maixiu are the six reserves with maximum ACMs, clustering in the east of TRHR except Yueguzonglie. This indicates the nearby regions are likely to have similar vegetation change.

The reserve and the non-reserve are compared in Table 2. Regarding the averaged ACM and the proportion of the positive pixels, a general recovery was found in the reserve with 0.0007 and 54.4%, respectively, and an overall slight degradation was found in the non-reserve with −0.0002 and 48.5%, respectively. We may conclude that 'The Project' has a positive but insignificant effect on the vegetation recovery in the reserve. Significant degradation remains in reserves including Dongzhong, Aangsai, Baizha, Tongtian River and Nianbaoyuze, as well as the border area of Zhiduo, Qumalai, Yushu and Zaduo which is ouside the reserve. Hereby we highlight the necessity of sustained vegetation and ecosystem conservation efforts in these regions.

5. Discussion

Currently, the widely used long-term NDVI datasets are primarily based on Advanced Very High Resolution Radiometer (AVHRR), SPOT-VEGETATION and MODIS sensors (Fensholt et al., 2009). The former two are based upon multiple platform/sensor systems. Tian

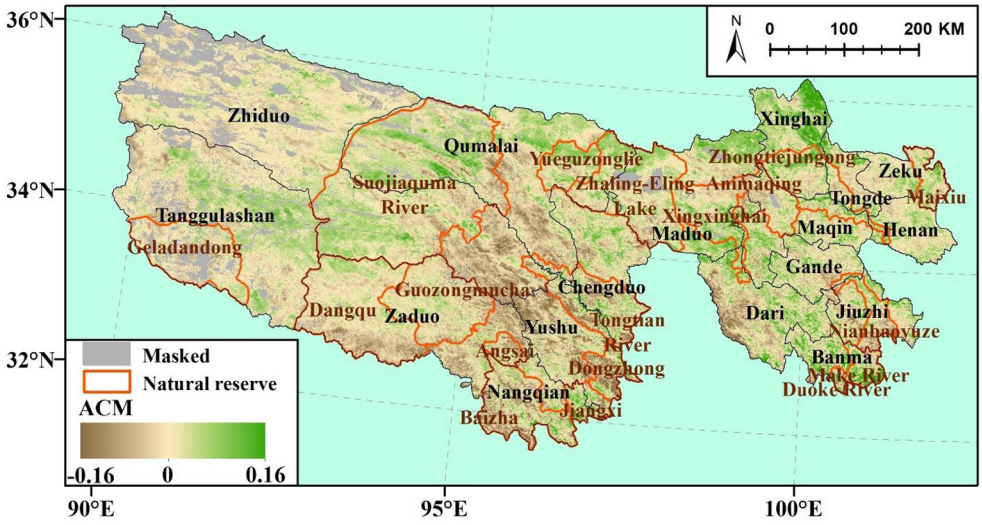

Fig. 5. The accumulated change magnitude (ACM) of TRHR from the third ten-day of February 2005 to the second ten-day of February 2015.

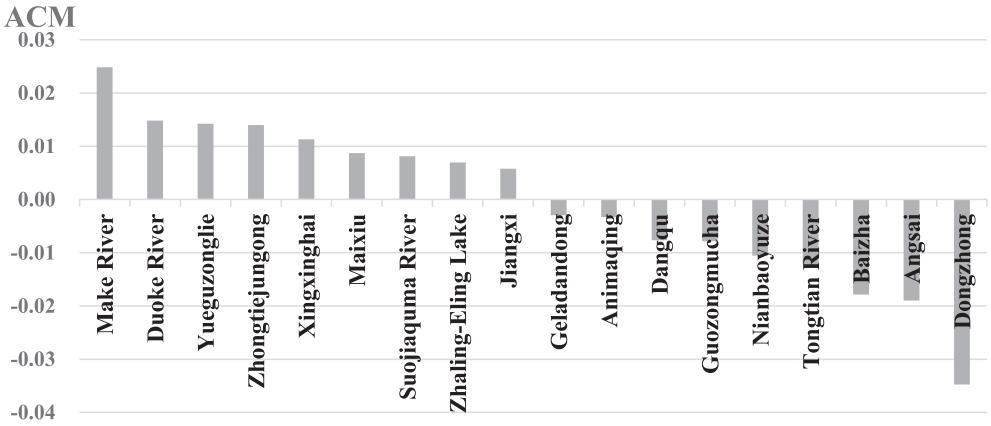

Fig. 6. The accumulated change magnitudes (ACMs) of 18 reserves.

Table 2
Statistics of the accumulated change magnitudes (ACMs) of the TRHR, the reserve and the non-reserve.

Region	Valid pixels	Averaged ACM	The proportion of the pixels which are	
			> 0	< 0
TRHR	918,705	0.0002	53.2%	46.8%
Reserve	392,949	0.0007	54.4%	45.6%
Non-reserve	525,756	−0.0002	48.5%	51.5%

et al. (2015) evaluated the temporal consistency of these datasets and revealed that the platform/sensor changes in AVHRR and SPOT-VEGETATION caused significant shifts in time series, and these shifts will possibly be detected and misleadingly treated as vegetation changes. Unlike AVHRR and SPOT-VEGETATION datasets, MODIS time series are based on single sensor and therefore not influenced by platform/sensor shift, for example, Terra-MOIDS MOD09GA surface reflectance dataset (Vermote et al., 2011). Moreover, the MODIS NDVI dataset has relatively high spatial resolution from 250 m to 1 km and sufficient temporal resolution from 8-day to 16-day. Hence, the MODIS NDVI dataset is applicable in vegetation analysis and has been widely used (Fensholt et al., 2009; Jacquin et al., 2010). However, Sun et al. (2016) urged caution in the interpretation of NDVI since it cannot reflect changes in vegetation species and community structure, and therefore relating NDVI changes to ecosystem changes is not straightforward.

The presented methodology based on the DBEST algorithm is more flexible than previous linear methods (Li et al., 2011; Liu et al., 2014; Liu and Shao, 2014; Sun et al., 2016; Zhang et al., 2016), concerning detecting spatio-temporal vegetation changes. In addition, it takes seasonal variation into account. Still, there is an agreement with the aforementioned studies, that is a general increasing trend of the vegetation in TRHR since 2000 was found (Table 3), but except Zhang et al. (2016). The discrepancy could be attributed to the adoption of NPP as the indicator. Vegetation coverage actually is a linear transformation of NDVI and thus an agreement is observed (Liu and Shao, 2014). However, when retrieving NPP using Carnegie–Ames–Stanford approach (CASA) model with inputs of NDVI and climate data, it is a non-linear and complex function of NDVI.

In principle, DBEST can also be employed to other climatic, ecological and anthropogenic factors related to vegetation changes. An integrated analysis of these aspects will definitely enhance our understanding of the complex relationship of vegetation with climate and human activities. However, DBEST is more appropriate for seasonal time series than deseasonalized time series. Only if the latter do not include high frequency variations, can DBEST be applied to them (Jamali et al., 2015). Additionally, these factors should be observed frequently enough, e.g. monthly observation. These two prerequisites restrain the application of DBEST to the indicators such as grazing area, and the number of livestock. Some indicators particularly NPP and precipitation are promising as the input data of DBEST to investigate the ecological productivity and climate conditions, respectively, which future studies should focus on.

Climate was suggested as the principal factor determining the vegetation changes in TRHR (Li et al., 2011; Sun et al., 2016; Zheng et al., 2017) and thus its effect should be removed to show the contribution of 'The Project'. Even though the positve effect of 'The Project' is in agreement with previous studies (Cai et al., 2015; Jiang and Zhang, 2016; Shao et al., 2017b), the methodology varies. Cai et al. (2015) established a linear relationship between NDVI and climate variables including temperature and precipitation, to predict the climate-induced NDVI. The residuals (the deviation between predicted NDVI and observed NDVI) were then calculated to represent the project-induced NDVI. Nevertheless, Zheng et al. (2017) noted that linear regression tools, when being used to simulate the relationship between climate and vegetation, would result in high uncertainties because the vegetation response to climate change is complex and non-linear (Lambin and Ehrlich, 1997). In line with Shao et al. (2017b), a comparison between

Table 3
A comparison with previous studies of the long-term vegetation trend in TRHR.

Reference	Indicator	Sensor	Time span	Trend
This study	NDVI	MODIS	2000–2015	A general increasing trend at a rate of 0.02
Sun et al. (2016)	NDVI	MODIS	2000–2013	A general increasing trend at a rate of 0.012
Li et al. (2011)	NDVI	SPOT-VEGETATION	2001–2010	A general increasing trend at a rate of 0.004
Liu et al. (2014)	NDVI	MODIS	2000–2011	A general increasing trend at a rate of 1.2%/10a
Liu and Shao (2014)	Vegetation coverage	SPOT-VEGETATION	1998–2012	A significant increasing trend ($p = 0.01$) at a rate of 0.004
Zhang et al. (2016)	NPP	AVHRR for 1982–2000, and MODIS for 2001–2012	1982–2012	A general increasing trend at a rate of 1.31 $g\,cm^{-2}\,yr^{-2}$, at the time scale of the entire time span An insignificant decreasing trend at a rate of $-0.24\,g\,cm^{-2}\,yr^{-2}$, at the time scale of the period from 2001 to 2012

the reserve and the non-reserve was made in this study. Specifically, the ACMs inside and outside the reserve were compared to confirm the effectiveness of 'The Project' on the vegetation recovery. However, we should note this comparison is based on an assumption of a similar climate contribution inside and outside the reserve.

It is well accepted that the TRHR was getting warmer and wetter in the past two decades (Dou, 2016; Tang et al., 2016), leading to an overall vegetation recovery to a large extent. However, this places a conflict with the negative ACM at −0.0002 of non-reserve (Table 2). A plausible explanation is that the implementation of 'The Project' strictly limited human disturbances to vegetation such as grazing. It was reported that around 50,000 local residents were encouraged to move out from the reserve and relocate in nearby towns (Cai et al., 2015), potentially having a negative effect on the vegetation outside the reserve.

In agreeement with Shao et al. (2017b), a positive but insignificant effect of 'The Project' was revealed in this study. A possible reason is that, although its total implementation area is 152,000 km^2, the area affecting vegetation coverage is only 514 km^2, merely taking up 0.34% of the entire reserve (Sun et al., 2016). Another explanation as Li et al. (2011) and Jiang and Zhang (2016) concluded is its uneven implementation with a short-term design. Shao et al. (2017a) summarized that, in the first stage of 'The Project', the ecosystem degradation was initially curbed and partially improved, but it was still far from the ideal state. Hereby we place special emphasis on the long-term and forward-looking planning of future projects to promote a fundamental recovery of the ecosystem.

6. Conclusions

In this study, we detected the vegetation changes of TRHR and further assessed the effects of 'The Project' on vegetation changes, using DBEST and MODIS NDVI dataset. The results indicate that the vegetation shows a gradually increasing trend with NDVI magnitude from around 0.24 in 2000 to 0.26 in 2015. The averaged ACM of TRHR is 0.033 and almost 90% area underwent recoveries, but meantime with some degraded areas distributed mainly in Maduo, Zaduo, Jiuzhi and Zhiduo. Through the comparison of the vegetation changes inside and outside the reserve during 2005–2015, we evaluated the influence of 'The Project' on the vegetation in the reserve. The slightly higher ACM of the reserve indicates it has a positive but insignificant influence on the vegetation recovery. Despite the implementation of 'The Project', there are several reserves with minus ACMs less than −0.01, including Dongzhong, Aangsai, Baizha, Tongtian River and Nianbaoyuze. In addition, the non-reserve region located in the border area of Zhiduo, Qumalai, Yushu and Zaduo was also found severely degradaded. All in all, whilst TRHR underwent a general recovery from 2000 to 2015, this area is still faced with a challenging future due to the progressive fluctuations of trend observed in this study. Hereby we highlight the necessity of sustained vegetation and ecosystem conservation efforts in this region.

Acknowledgments

The authors thank the Geospatial Data Cloud (http://www.gscloud.cn/), as well as the Chinese Academy of Environmental Science data center (http://www.resdc.cn) for providing valuable datasets. The authors are also grateful to Dawei Ma, Xun Hu, Ruonan Qiu and Lingjie Liu for their work in data preparation and preprocessing. This work was supported by the National Nature Science Foundation of China (No. 41271361) and the Key Projects of the National Science and Technology Pillar Program during the Twelfth Five-Year Plan Period (No. 2013BAC03B04).

References

Cai, H., Yang, X., Xu, X., 2015. Human-induced grassland degradation/restoration in the central Tibetan Plateau: the effects of ecological protection and restoration projects. Ecol. Eng. 83, 112–119.

Cleveland, R.B., Cleveland, W.S., 1990. STL: a seasonal-trend decomposition procedure based on loess. J. Off. Stat. 6, 3–33.

de Jong, R., Verbesselt, J., Schaepman, M.E., de Bruin, S., 2012. Trend changes in global greening and browning: contribution of short-term trends to longer-term change. Global Change Biol. 18, 642–655.

Dou, R., 2016. The climate change and adaptation strategies for sustainable development in the Three-River Headwaters Region in Qinghai Province in recent half century. Ecol. Econ. 32, 165–171 (in Chinese).

Fensholt, R., Rasmussen, K., Nielsen, T.T., Mbow, C., 2009. Evaluation of earth observation based long term vegetation trends – Intercomparing NDVI time series trend analysis consistency of Sahel from AVHRR GIMMS, Terra MODIS and SPOT VGT data. Remote Sensing Environ. 113, 1886–1898.

Gu, J., Li, X., Huang, C., 2010. Land cover classification based on time-series MODIS NDVI data in Heihe River Basin. Adv. Earth Sci. 25, 317–326 (in Chinese).

Jacquin, A., Sheeren, D., Lacombe, J.-P., 2010. Vegetation cover degradation assessment in Madagascar savanna based on trend analysis of MODIS NDVI time series. Int. J. Appl. Earth Observ. Geoinform. 12, S3–S10.

Jamali, S., Jönsson, P., Eklundh, L., Ardö, J., Seaquist, J., 2015. Detecting changes in vegetation trends using time series segmentation. Remote Sensing Environ. 156, 182–195.

Jamali, S., Seaquist, J., Eklundh, L., Ardö, J., 2014. Automated mapping of vegetation trends with polynomials using NDVI imagery over the Sahel. Remote Sensing Environ. 141, 79–89.

Jiang, C., Zhang, L., 2016. Ecosystem change assessment in the Three-river Headwater Region, China: patterns, causes, and implications. Ecol. Eng. 93, 24–36.

Lambin, E.F., Ehrlich, D., 1997. Land-cover changes in sub-saharan Africa (1982–1991): application of a change index based on remotely sensed surface temperature and vegetation indices at a continental scale. Remote Sensing Environ. 61, 181–200.

Li, H., Liu, G., Fu, B., 2011. Response of vegetation to climate change and human activity based on NDVI in the Three-River Headwaters region. Acta Ecol. Sin. 31, 5495–5504 (in Chinese).

Liu, J., 1997. Study on national resources & environment survey and dynamic monitoring using remote sensing. J. Remote Sensing 1, 225–230 (in Chinese).

Liu, J., Xu, X., Shao, Q., 2008. The spatial and temporal characteristics of grassland degradation in the Three-River Headwaters Region in Qinghai Province. Acta Geogr. Sin. 63, 364–376 (in Chinese).

Liu, X.F., Zhang, J.S., Zhu, X.F., Pan, Y.Z., Liu, Y.X., Zhang, D.H., Lin, Z.H., 2014. Spatiotemporal changes in vegetation coverage and its driving factors in the Three-River Headwaters Region during 2000–2011. J. Geogr. Sci. 24, 288–302.

Liu, Z., Shao, Q., 2014. The fractional vegetation cover change and its response to climate change in Three-River Headwaters region. Res. Soil Water Conserv. 21, 334–339 (in Chinese).

Montandon, L.M., Small, E.E., 2008. The impact of soil reflectance on the quantification of the green vegetation fraction from NDVI. Remote Sensing Environ. 112, 1835–1845.

Parmesan, C., Yohe, G., 2003. A globally coherent fingerprint of climate change impacts across natural systems. Nature 421, 37.

PGQP (The Peolple's Government of Qinghai Province), 2013. The Planning on Ecological Protection and Construction II in the TRHR Nature Reserve. Avaliable online: http://www.ndrc.gov.cn/zcfb/zcfbtz/201404/W020140411568698686984.pdf (in Chinese).

Purevdorj, T., Tateishi, R., Ishiyama, T., Honda, Y., 1998. Relationships between percent vegetation cover and vegetation indices. Int. J. Remote Sensing 19, 3519–3535.

Schwarz, G., 1978. Estimating the dimension of a model. Ann. Stat. 6, 15–18.

Shao, J.A., Shao, Q.Q., Liu, J.Y., 2009. Soil property and its formation of ecosystems in three river sources, Qinghai. Geogr. Res. 28, 613–624 (in Chinese).

Shao, Q., Fan, J., Liu, J., Huang, L., Cao, W., Liu, L., 2017a. Target-based assessment on effects of first-stage ecological conservation and restoration project in three-river source region, China and policy recommendations. Bull. Chin. Acad. Sci. 32, 35–44.

Shao, Q., Cao, W., Fan, J., Huang, L., Xu, X., 2017b. Effects of an ecological conservation and restoration project in the Three-River Source Region, China. J. Geogr. Sci. 27, 183–204.

Sitch, S., Smith, B., Prentice, I.C., Arneth, A., Bondeau, A., Cramer, W., Kaplan, J.O., Levis, S., Lucht, W., Sykes, M.T., Thonicke, K., Venevsky, S., 2003. Evaluation of ecosystem dynamics, plant geography and terrestrial carbon cycling in the LPJ dynamic global vegetation model. Global Change Biol. 9, 161–185.

Sun, Q., Li, B., Xu, L., Zhang, T., Ge, J., Li, F., 2016. Analysis of NDVI change trend and its impact factors in the Three-River Headwater Region from 2000 to 2013. J. Geo-Inform. Sci. 18, 1707–1716 (in Chinese).

Tang, M., Zhang, B., Zhang, Y., Ji, D., Ma, Q., Zhang, G., 2016. Characteristics of temporal and spatial variations of Surface Aridity Index and climatic factors on the impact in Headwaters of the Three Rivers in recent 55 years. Ecol. Environ. Sci. 25, 248–259 (in Chinese).

Tian, F., Fensholt, R., Verbesselt, J., Grogan, K., Horion, S., Wang, Y., 2015. Evaluating temporal consistency of long-term global NDVI datasets for trend analysis. Remote Sensing Environ. 163, 326–340.

Tong, L., Xu, X., Fu, Y., Li, S., 2014. Wetland changes and their responses to climate change in the "Three-River Headwaters" Region of China since the 1990s. Energies 7, 2515–2534.

Vermote, E.F., Kotchenova, S.Y., Ray, J.P., 2011. MODIS Surface Reflectance User's Guide. MODIS Land Surface Reflectance Science Computing Facility.

Xu, W., Gu, S., Zhao, X.Q., Xiao, J., Tang, Y., Fang, J., Zhang, J., Jiang, S., 2011. High positive correlation between soil temperature and NDVI from 1982 to 2006 in alpine meadow of the Three-River Source Region on the Qinghai-Tibetan Plateau. Int. J.

Appl. Earth Observ. Geoinform. 13, 528–535.
Xu, X., Liu, J., Shao, Q., Fan, J., 2008. The dynamic changes of ecosystem spatial pattern and structure in the Three-River Headwaters region in Qinghai Province during recent 30 years. Geogr. Res. 27 829–838 + 974 (in Chinese).
Zhang, Y., Zhang, C., Wang, Z., Chen, Y., Gang, C., An, R., Li, J., 2016. Vegetation dynamics and its driving forces from climate change and human activities in the Three-River Source Region, China from 1982 to 2012. Sci. Total Environ. 563–564, 210–220.
Zhang, Y., Zhang, S., Zhai, X., 2012. Runoff variation and its response to climate change in the Three Rivers Source Region. J. Geogr. Sci. 22, 781–794.
Zhao, N., 2014. The second-stage of the TRHR ecological conservation and restoration project starts. Resour. Hum. Settlements 48 (in Chinese).
Zheng, Y., Han, J., Huang, Y., Fassnacht, S.R., Xie, S., Lv, E., Chen, M., 2017. Vegetation response to climate conditions based on NDVI simulations using stepwise cluster analysis for the Three-River Headwaters region of China. Ecol. Indic (In press).